# Vibrational Study of Multiply Metal-Metal Bonded Ruthenium Porphyrin Dimers

**C. Drew Tait,[†] James M. Garner,[‡] James P. Collman,*[,‡] Alfred P. Sattelberger,*[,†] and William H. Woodruff*[,†]**

*Contribution from the Inorganic and Structural Chemistry Group (INC-4), Isotope and Nuclear Chemistry Division, Los Alamos National Laboratory, Los Alamos, New Mexico 87545, and the Department of Chemistry, Stanford University, Stanford, California 94305.*
*Received December 20, 1988*

**Abstract:** The resonance Raman scattering (RR) and infrared absorption (IR) spectra of the $\{[Ru(OEP)]_2\}^{n+}$ complexes (OEP = 2,3,7,8,12,13,17,18-octaethylporphyrin dianion; $n$ = 0, 1, 2; Ru-Ru bond order = 2.0, 2.5, 3.0) have been investigated. Resonance Raman studies revealed the Ru-Ru stretch to increase in frequency upon oxidation [285 $cm^{-1}$ ($n$ = 0), 301 $cm^{-1}$ ($n$ = 1), and 310 $cm^{-1}$ ($n$ = 2)], consistent with the removal of electrons from $\pi^*$ metal-metal antibonding orbitals. The porphyrin-centered vibrational modes (both RR and IR active) for the complexes are essentially independent of oxidation state and very similar to those found for the monomeric complex Ru(OEP)(CO)(L). These data are likewise consistent with oxidation of metal-metal antibonding electrons. Correlations between the RR frequencies and empirical structural parameters for the complexes (Ru-Ru and Ru-N bond distances) are made and compared to the X-ray structure previously determined for the neutral species. From these correlations, the Ru-Ru bond distance decreases from 2.39 to 2.33 and 2.30 Å upon successive oxidation, while the porphyrin core size (nitrogen to porphyrin center) remains constant at ca. 2.04 Å. No vibrational evidence for direct intradimer coupling between the $\pi$ orbitals of the bound porphyrin rings is found.

A common problem encountered in the study of binuclear transition-metal complexes that contain unbridged metal-metal multiple bonds is the inability of monodentate and bidentate ligands to remain inert when the dimers are oxidized or reduced.[1-3] Ligand lability in the redox partners can lead to higher nuclearity clusters, bridges across the metal-metal bond, or substitutions that obfuscate changes in metal-metal bonding as a function of electronic configuration. Binuclear transition-metal systems incorporating the 2,3,7,8,12,13,17,18-octaethylporphyrin dianion (OEP) circumvent these problems because this rigid, tetradentate, square-planar ligand is incapable of bridging two metals and its steric properties restrict the formation of higher nuclearity clusters.[4] Investigation of the chemical and physical properties of metalloporphyrin dimers is also important because of possible similarities to the "special pair" of bacteriochlorophylls in reaction centers, which figure prominently in the initial stages of photosynthesis.[5,6] In addition, the development of models for efficient electron conductivities in stacked $\pi$-system aggregates is enhanced by an understanding of the electronic properties of analogous dimers.[7]

Opportunities to address all of these issues are provided by a systematic examination of the resonance Raman (RR) and infrared absorption (IR) spectra of the $\{[Ru(OEP)]_2\}^{n+}$ series, where $n$ = 0, 1, or 2. A previous X-ray structural determination of the neutral compound[8] provides a starting point from which to study the vibrational spectra. The two ruthenium atoms are separated by 2.408 (1) Å, and each ruthenium lies 0.30 Å above its porphyrin nitrogen plane toward the other metal. The mean distance between the essentially planar porphyrin skeletons is 3.26 Å, and the porphyrin cores are twisted by 23.8°. The molecular orbital energy diagram shown in Figure 1 has been advanced to explain the metal-metal bonding, as well as the magnetic ($^1H$ NMR and magnetic susceptibility)[8,9] and electrochemical[9] properties of paramagnetic $\{[Ru(OEP)]_2\}^0$ and $\{[Ru(OEP)]_2\}^{1+}$ and diamagnetic $\{[Ru(OEP)]_2\}^{2+}$. The electronic configuration of the neutral dimer is $\sigma^2\pi^4\delta^2\delta^{*2}\pi^{*2}$, resulting in a formal metal-metal bond order of 2. Successive oxidations remove the two $\pi^*$ electrons, increasing the bond order to 2.5 and 3. RR spectroscopy is an effective probe for symmetric metal-metal stretches[10,11] and is employed here to obtain direct evidence for changes in bond order/bond length.

RR spectroscopy of porphyrin macrocycles is a well-developed method[10-14] for probing porphyrin structural features and, in conjunction with IR spectroscopic measurements, the extent of $\pi$ interaction between two cofacially bound macrocycles.[15-21] Different vibrational modes are sensitive to the extent of metal-to-porphyrin $\pi$ back-bonding, the size of the porphyrin core, and overlap between the $\pi$ systems of adjacent porphyrin rings. The latter can range from full delocalization of cation holes over both ligands, as reported for porphyrin-oxidized cerium(IV) bis(OEP) and tetraphenylporphyrin (TPP) sandwich complexes,[19] to weaker exciton coupling in, e.g., free base etioporphyrin[22] and Sc-O-Sc porphyrin dimers,[23] to, finally, systems that show no

[†] Los Alamos National Laboratory.
[‡] Stanford University.

(1) Cotton, F. A.; Walton, R. A. *Multiple Bonds Between Metal Atoms*; Wiley: New York, 1982.
(2) *Inorganic Chemistry: Toward the 21st Century*; Chisholm, M. H., Ed.; ACS Symposium Series 211; American Chemical Society; Washington, DC, 1983.
(3) Recent Advances in the Chemistry of Metal-Metal Multiple Bonds. Chisholm, M. H., Ed. *Polyhedron* **1987**, *6*, 667-801.
(4) Collman, J. P.; Barnes, C. E.; Woo, L. K. *Proc. Natl. Acad. Sci. U.S.A.* **1983**, *80*, 7684-7688.
(5) *The Porphyrins*; Dolphin, D., Ed.; Academic Press: New York, 1979; Vol. I-VII.
(6) *Porphyrins: Excited States and Dynamics*; Gouterman, M., Rentzepis, P. M., Straub, K. D., Eds.; ACS Symposium Series 321; American Chemical Society: Washington, DC, 1986.
(7) Hoffman, B. M.; Ibers, J. A. *Acc. Chem. Res.* **1983**, *16*, 15-21.
(8) Collman, J. P.; Barnes, C. E.; Swepston, P. N.; Ibers, J. A. *J. Am. Chem. Soc.* **1984**, *106*, 3500-3510.
(9) Collman, J. P.; Prodolliet, J. W.; Leidner, C. R. *J. Am. Chem. Soc.* **1986**, *108*, 2916-2921.
(10) Clark, R. J. H.; Stewart, B. *Struct. Bonding* **1979**, *36*, 1-80.
(11) Clark, R. J. H.; Dines, T. J. *Angew. Chem., Int. Ed. Engl.* **1986**, *25*, 131-158.
(12) Bernstein, H. J. *Philos. Trans. R. Soc. London, A* **1979**, *293*, 287-302.
(13) Kitagawa, T.; Abe, M.; Ogoshi, H. *J. Chem. Phys.* **1978**, *69*, 4516-4525.
(14) Abe, M.; Kitagawa, T.; Kyogoku, Y. *J. Chem. Phys.* **1978**, *69*, 4526-4534.
(15) Adar, F.; Srivastava, T. S. *Proc. Natl. Acad. Sci. U.S.A.* **1975**, *72*, 4419-4424.
(16) Burke, J. M.; Kincaid, J. R.; Spiro, T. G. *J. Am. Chem. Soc.* **1978**, *100*, 6077-6083.
(17) Schick, G. A.; Bocian, D. F. *J. Am. Chem. Soc.* **1983**, *105*, 1830-1838.
(18) Hofmann, J. A.; Bocian, D. F. *J. Phys. Chem.* **1984**, *88*, 1472-1479.
(19) (a) Donohoe, R. J.; Duchowski, J. K.; Bocian, D. F. *J. Am. Chem. Soc.*, in press. (b) Yan, X.; Holten, D. *J. Phys. Chem.* **1988**, *92*, 409-414.
(20) (a) Shelnutt, J. A.; Dobry, M. M.; Satterlee, J. D. *J. Phys. Chem.* **1984**, *88*, 4980-4987. (b) Shelnutt, J. A. *J. Phys. Chem.* **1984**, *88*, 4988-4992.
(21) Shelnutt, J. A. *J. Phys. Chem.* **1983**, *87*, 605-616.
(22) Selensky, R.; Holten, D.; Windsor, M. W.; Paine, J. B., III; Dolphin, D.; Gouterman, M.; Thomas, J. C. *Chem. Phys.* **1981**, *60*, 33-46.

0002-7863/89/1511-7806$01.50/0 © 1989 American Chemical Society

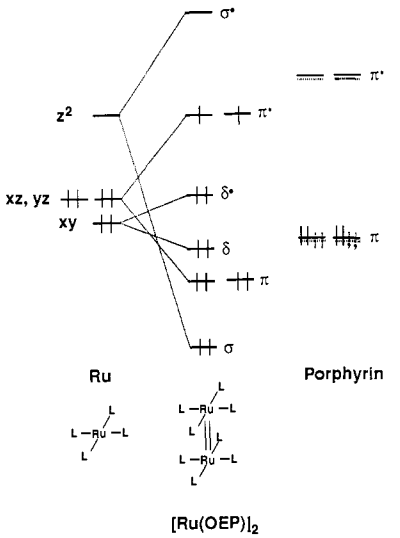


**Figure 1.** Molecular orbital diagram outlining the orbital parentage of the metal-metal bonds and their energies relative to the porphyrin orbitals.

vibrational evidence for orbital overlap, such as those containing Fe-O-Fe or Fe-N-Fe bridges.[16-18] Porphyrin vibrations of the $\{[Ru(OEP)]_2\}^{n+}$ complexes are also reported herein and discussed in the aforementioned context.

## Experimental Section

The air-sensitive ruthenium(II,II) dimer was synthesized as previously described.[8] Stoichiometric amounts of $AgBF_4$ were added to the neutral dimer to prepare samples of $\{[Ru(OEP)]_2\}(BF_4)$ and $\{[Ru(OEP)]_2\}(BF_4)_2$.[9] Ru(OEP)(CO) was purchased from Aldrich and used wihout further purification. Tetrahydrofuran (THF) and toluene were distilled from Na/K alloy and stored in a Vacuum Atmospheres inert-atmosphere glovebox. The neutral dimer is unstable in chlorinated solvents and in moderately to strongly coordinating solvents, so THF was chosen for the Raman experiments. While the monocation dimer is soluble in THF, the dication dimer is not. Fortunately, the cationic dimers are both soluble and stable in chlorinated solvents, allowing the use of methylene chloride and chloroform-*d*, both of which contain fewer obscuring solvent vibrational bands than THF. The latter solvents were dried with $P_2O_5$, distilled, and stored in the glovebox. RR samples prepared in the glovebox were sealed with a Teflon vacuum stopcock, removed from the box, subjected to a freeze-pump-thaw cycle, and flame sealed. IR samples prepared in the glovebox were sealed in KBr or NaCl cavity cells (0.1-mm path length) equipped with a vacuum-tight Teflon stopper and holder (Spectra-Tech).

Excitation for the RR experiments was provided by $Ar^+$ and $Kr^+$ ion lasers (Spectra Physics Models 171 and 2025). To minimize photodecomposition, samples were cooled to ca. −10 °C with a circulating antifreeze bath, and the laser power was reduced to 10 mW when exciting into the Soret and 30 mW elsewhere. The excitation was line-focused to further reduce the power density at the sample. Scattered light was focused into either a SPEX or an Instruments SA/Jobin Yvon scanning double monochromator (slits set to 3-5 $cm^{-1}$ resolution; frequency precision for strong peaks ±2 $cm^{-1}$). Because the precision of the depolarization ratios ($\rho$) obtained was only ±0.1, only general information such as whether bands were polarized ($a_{1g}$ modes), depolarized ($b_{1g}$ and $b_{2g}$ modes), or anomalously polarized ($a_{2g}$ modes) could be determined. Any *z* component (i.e., along the Ru-Ru axis) to the absorption giving rise to the resonant enhancement could not be inferred from deviation of $\rho$ from 0.125 for the symmetric modes.[17]

Infrared absorption measurements were performed with a Digilab FTS-40 FTIR at 2-$cm^{-1}$ resolution, employing triangular apodization, and signal averaging over 1920 scans.

## Results and Discussion

**I. Resonance Raman Studies.** The electronic absorption spectra of $\{[Ru(OEP)]_2\}^{n+}$ ($n$ = 0, 1, or 2) have been published previously[9] and are reproduced here (Figure 2) to show the bands that give rise to the RR enhancements. Compared to the spectrum of Ru(OEP)(CO), both the Soret bands and the Q bands are blue

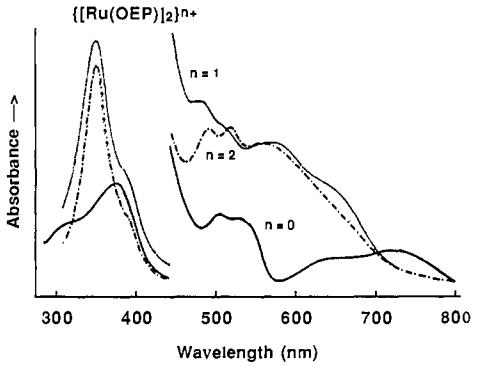


**Figure 2.** Absorption spectra for $\{[Ru(OEP)]_2\}^{n+}$ in benzene (—, $n$ = 0), $CH_2Cl_2$ (···, $n$ = 1), and $CH_2Cl_2$ (—·—, $n$ = 2). From ref 9.

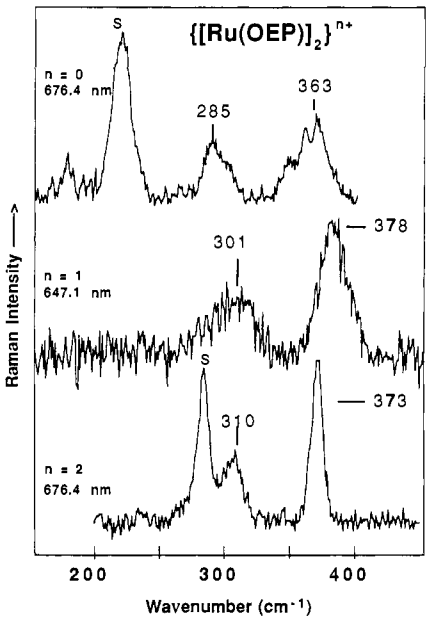


**Figure 3.** Low-frequency RR spectra upon red excitation of $\{[Ru(OEP)]_2\}^{n+}$ ($n$ = 0, in toluene; $n$ = 1, in THF; $n$ = 2, in $CH_2Cl_2$). Note that different solvents were required from considerations of sample solubility, sample stability, and the avoidance of interfering solvent Raman peaks. All three spectra are base-line corrected.

shifted in the dimeric species, perhaps as a result of excitonic splitting of the porphyrin-centered excited states.[4,9,22-25] In addition, an entirely new absorbance region appears in the neutral dimer in the 600-800-nm range, shifting to higher energy for the oxidized dimers. The dimer RR studies are conveniently categorized by reference to the region of the electronic spectrum used for laser excitation: the dimer absorptions at long wavelengths, the Soret-band region of the porphyrin, and the Q-band region of the porphyrin.

Excitation into the long-wavelength absorption region of the ruthenium dimers, transitions that presumably involve the metal-metal (anti)bonding orbitals, was performed to determine the Ru-Ru stretching frequencies. An estimate of the Ru-Ru stretching frequency for the neutral dimer was made to aid in the search. With the known 2.41-Å Ru-Ru distance,[8] a force constant of 2.32 mdyn/Å was estimated from empirical bond distance/force constant relationships.[26] This force constant was then used to estimate the Ru-Ru stretching frequency (279 $cm^{-1}$) via the diatomic approximation.[27] The spectra for $\{[Ru(OEP)]_2\}^{0,1+,2+}$

(23) Gouterman, M.; Holten, D.; Lieberman, E. *Chem. Phys.* **1977**, *25*, 139-153.

(24) Zgierski, M. Z. *Chem. Phys. Lett.* **1986**, *124*, 53-58.

(25) Exciton coupling need not be invoked to explain the blue shifts upon dimerization. At least some of the effect is from "solvent" interaction upon dimerization. See: Shelnutt, J. A. *J. Phys. Chem.* **1984**, *88*, 4988-4992.

(26) Miskowski, V. M.; Dallinger, R. F.; Christoph, G. G.; Morris, D. E.; Spies, G. H.; Woodruff, W. H. *Inorg. Chem.* **1987**, *26*, 2127-2132. The appropriate equation for elements Rb-Xe is: $r = 1.83 + 1.51 \exp(-k/2.48)$, where $r$ is in Å and $k$ is in mdyn/Å.

**Table I.** Structural Parameters Calculated from Observed Ru–Ru Stretching Frequencies

| | $\nu$(Ru–Ru), cm$^{-1}$ | $k$,[a] mdyn/Å | $D_{Ru-Ru}$,[b] Å | $D_{Ru-Ru}$,[c] Å |
|---|---|---|---|---|
| $\{[Ru(OEP)]_2\}^0$ | 285 | 2.42 | 2.39 | 2.41 |
| $\{[Ru(OEP)]_2\}^{1+}$ | 301 | 2.70 | 2.33 | |
| $\{[Ru(OEP)]_2\}^{2+}$ | 310 | 2.86 | 2.30 | |

[a] Calculated from the diatomic approximation (ref 27). [b] Calculated from empirical force constant–bond length correlations (ref 26). [c] X-ray structure determination (ref 8).

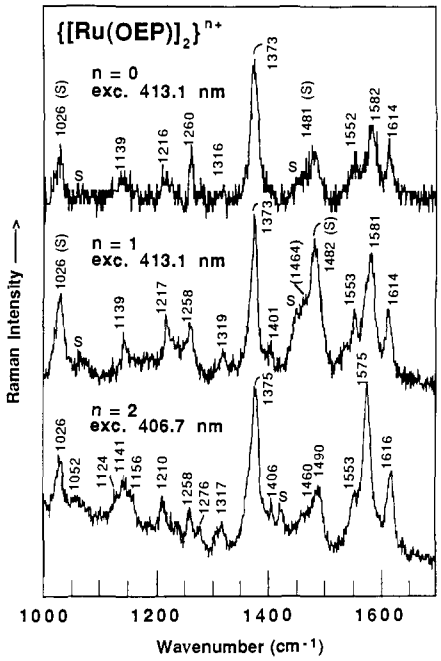


**Figure 4.** High-frequency RR spectra upon excitation into the red edge of the porphyrin Soret absorption. Solvents were THF for the $n = 0$ and $n = 1$ species and $CH_2Cl_2$ for the $n = 2$ species.

reveal a polarized Raman peak, which shifts from 285 cm$^{-1}$ in the neutral dimer to 301 cm$^{-1}$ in the monocation to 310 cm$^{-1}$ in the dication (Figure 3). We assign these as the Ru–Ru stretching vibrations. They are not present when exciting into the other porphyrin-centered absorption bands of the dimers or Ru(OEP)(CO) (vide infra). The breadth of these low-frequency modes suggests that they are composite features. Because there are eight ruthenium isotopes present in reasonable natural abundance (from mass 96 to 104),[28] the widths of the peaks support their assignment as the Ru–Ru stretches.

By use of the experimental values, Ru–Ru force constants and distances were back-calculated from the relationships mentioned above to give the metal–metal bond distance estimates presented in Table I. The increase in Ru–Ru force constant and decrease in metal–metal bond length upon oxidation are consistent with the orbital diagram shown in Figure 1, and successive removal of electrons from the $\pi^*$ metal–metal antibonding orbitals. Even though the molecular orbital diagram predicts that the removal of each electron should increase the formal bond order by an equal amount, the first oxidation appears to cause a larger change than the second. Other factors, such as increased porphyrin–porphyrin steric repulsions and contraction of the ruthenium 4d orbitals resulting in poorer $\sigma$, $\pi$, and $\delta$ bonding interactions upon oxidation, will oppose shortening of the Ru–Ru bond distance.[29]

(27) $k = (3.55 \times 10^{17})\mu\nu^2$, $k$ = force constant (in mdyn/Å); $\mu$ = reduced mass of the two Ru atoms (in g); $\nu$ = vibrational frequency (in cm$^{-1}$).

(28) *CRC Handbook of Chemistry and Physics*, Weast, R. C., Ed.; CRC Press: Boca Raton, Fl, 1985; pp B-277–B-288.

(29) Orbital contraction with increasing charge offsetting increases in formal bond order has been invoked previously to explain trends in the Re–Re bond lengths for the series $[Re_2Cl_4(PMe_2Ph)_4]^{0,1+,2+}$. See: Cotton, F. A.; Dunbar, K. R.; Falvello, L. R.; Tomas, M.; Walton, R. A. *J. Am. Chem. Soc.* **1983**, *105*, 4950–4954.

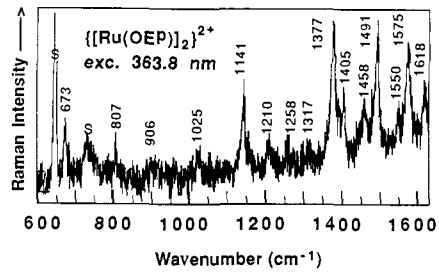


**Figure 5.** High-frequency RR spectrum for $\{[Ru(OEP)]_2\}^{2+}$ (in $CDCl_3$) upon excitation into the Soret maximum.

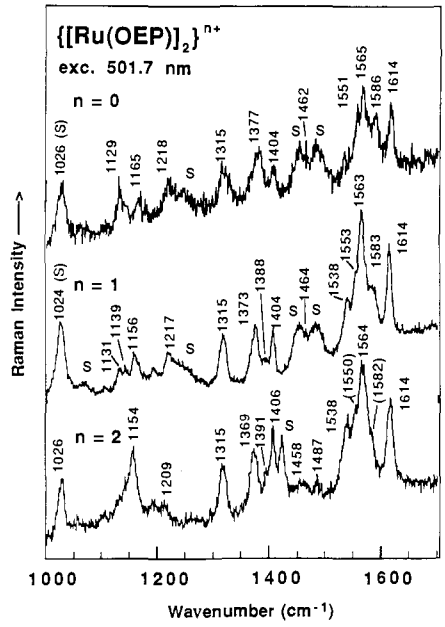


**Figure 6.** High-frequency RR spectra upon excitation into the porphyrin-based Q-band region. Solvents were THF for the $n = 0$ and $n = 1$ dimers and $CH_2Cl_2$ for the $n = 2$ dimer.

Another vibrational mode, found between 368 and 378 cm$^{-1}$, is strongly enhanced by excitation to the red of the Q bands, especially in the case of the cationic complexes. On the basis of its frequency and polarization, this Raman peak is assigned as $\nu_8$, an "in-plane" symmetric stretching vibration of the $RuN_4$ core. The coupling of the $\nu_8$ mode of $[(TPP)Fe]_2N$ with the Fe–N–Fe stretch has been demonstrated previously,[17] and the enhancement of $\nu_8$ in this case is likely a result of coupling to the Ru–Ru stretch.

Excitation into the porphyrin-based Soret and Q bands produces Raman scattering of the essentially in-plane porphyrin skeletal modes. Figures 4 and 5 show the results of excitation into the Soret bands for the three dimeric products, while Figure 6 shows the Raman spectra of the skeletal region obtained upon excitation into the Q-band region of the absorption spectra. As in previous dimeric porphyrin studies,[15-20] the vibrations can be described, to a first approximation, as in-plane skeletal modes of the corresponding monomer. Vibrational assignments of the porphyrin skeletal modes, shown in Table II, were inferred from the depolarization ratios and from comparisons with the vibrational spectra of Ni(OEP) and Ru(OEP)(CO).[30] The modes are classified in the $D_{4h}$ point group of the monomeric porphyrin moieties making up the dimer (vide infra). The Ni(OEP) compound is a useful standard for comparison because a complete normal coordinate analysis has been correlated with the spectra,[13,14] and the vibrational numbering scheme for OEP vibrations was developed for this compound.

Figure 4 shows the RR spectra obtained upon excitation into the red edge of the Soret. While $\{[Ru(OEP)]_2\}^{2+}$ exhibits a similar

(30) Kim, D.; Su, Y. O.; Spiro, T. G. *Inorg. Chem.* **1986**, *25*, 3993–3997.

**Table II.** Porphyrin RR Vibrational Assignments for Ru(OEP)(CO) and $\{[Ru(OEP)]_2\}^{n+}$

| monomer[a] | $n = 0$[b] | $n = 1$[b] | $n = 2$[b] | assignment[c] | |
|---|---|---|---|---|---|
| 1025 | 1027 | 1024 | 1026 | $\nu_5$ | $a_{1g}$ |
| 1125 | 1129 | 1122 | 1124 | ($\nu_{22}$ | $a_{2g}$) |
| 1138 | 1142 | 1140 | 1141 | ($\nu_6 + \nu_8$ | $a_{1g}$) |
| | | | | (and/or $\nu_{14}$ | $b_{1g}$) |
| 1165 | 1165 | 1163 | 1155 | ($\nu_{30}$ | $b_{2g}$) |
| 1214 | 1217 | 1216 | 1208 | $\nu_{13}$ | $b_{1g}$ |
| 1257 | 1259 | | 1258 | $\nu_5 + \nu_9$ | $a_{1g}$ |
| 1270 | | | 1276 | $\nu_{15} + \nu_{33}$ | $a_{1g}$ |
| 1314 | 1316 | 1318 | 1317 | $\nu_{21}$ | $a_{2g}$ |
| 1363 | | 1365 | 1369 | $\nu_{12}$ | $b_{1g}$ |
| 1371 | 1375 | 1375 | 1375 | $\nu_4$ | $a_{1g}$ |
| 1383 | | 1388 | | $\nu_{20}$ | $a_{2g}$ |
| 1400 | 1405 | 1404 | 1406 | $\nu_{29}$ | $b_{2g}$ |
| 1449 | 1460 | | 1458 | ($\nu_{28}$ | $b_{2g}$) |
| 1475 | 1485 | 1482 | 1490 | $\nu_3$ | $a_{1g}$ |
| | | 1538 | 1538 | | |
| 1548 | 1553 | 1553 | 1551 | $\nu_{11}$ | $b_{1g}$ |
| 1559 | 1565 | 1562 | 1565 | $\nu_{19}$ | $a_{2g}$ |
| 1579 | 1582 | 1578 | 1575 | $\nu_2$ | $a_{1g}$ |
| 1609 | 1614 | 1615 | 1616 | $\nu_{10}$ | $b_{1g}$ |

[a] Ru(OEP)(CO) in $CH_2Cl_2$ (ref 29). [b] Solvents used: $n = 0$, THF; $n = 1$, THF, $CH_2Cl_2$, $CDCl_3$; $n = 2$, $CH_2Cl_2$, $CDCl_3$. [c] Assignments in parentheses are tentative due to lack of intensity, and hence lack of depolarization ratio, of the Raman band. Vibrational band numbering corresponds to that of ref 13 and 14.

spectrum upon excitation near the Soret maximum (363.8-nm excitation, Figure 5), $\{[Ru(OEP)]_2\}^{1+}$ is photooxidized (the 1216-$cm^{-1}$ peak shifts to 1208 $cm^{-1}$) upon excitation at the same wavelength, even at low (< 10-mW) excitation power. Note that none of the bands is shifted significantly from its corresponding position in the spectrum of monomeric Ru(OEP)(CO). Such a result has precedent. The vibrational peak positions of stacked silicon phthalocyanines, for example, are similar to those of silicon phthalocyanine monomer and to other stacked silicon phthalocyanines of different aggregation.[31] As the Soret is an intense, electronically allowed band, totally symmetric porphyrin modes are expected to dominate the Soret-excited RR spectrum.[10-12] However, several bands that are not totally symmetric [e.g., 1615 $cm^{-1}$ ($b_{1g}$), 1553 $cm^{-1}$ ($b_{1g}$), 1317 $cm^{-1}$ ($a_{2g}$), and 1216 $cm^{-1}$ ($b_{1g}$); see Table II] are nonetheless observed upon excitation into the Soret band (Figure 4). An excited-state geometry change is an unlikely explanation for A-term enhancement of these modes because the overall symmetry of the molecule would have to be reduced to $C_2$ (all the modes must be totally symmetric in the common group).[11] While Jahn–Teller effects can give A-term enhancement to nontotally symmetric modes, $a_{2g}$ modes are not Jahn–Teller active in porphyrins.[10,11] Alternatively, an underlying, unresolved absorption that receives intensity from vibronic coupling to the Soret may contribute through a Herzberg–Teller (B-term) mechanism. A charge-transfer band [ligand-to-metal (LMCT) or metal-to-ligand (MLCT)] may exist in this spectral region. Like the Soret and Q bands, these would also be E transitions ($x$, $y$ polarized; see Figure 1) and, like the Q band, may gain some intensity from vibronic coupling with the Soret, especially since the energy difference between them is small.

Excitation throughout the Q-band region of the $\{[Ru(OEP)]_2\}^{n+}$ complexes provides the spectra shown in Figure 6. Each of the vibrational modes seen in Ru(OEP)(CO) has a corresponding mode at similar frequency in the dimeric complexes (Table II). While no $H_4OEP^{2+}$, $H_3OEP^{1+}$, or $H_2OEP$ (common impurities in oxidized complexes)[32,33] was detected, the weak peak at 1538 $cm^{-1}$ is attributed to trace amounts of monomeric Ru(OEP). As observed in the RR spectra of Ru(OEP)(py)$_2$ (py = pyridine),[2,30,34] the band at 1535 $cm^{-1}$ is by far the strongest band when exciting into the Q-band region. No new vibrational band is found exclusively in the spectra of the dimeric compounds. Furthermore, no splitting of vibrational peaks was observed, but this could be a consequence of the spectrometer slit settings (4–5-$cm^{-1}$ resolution to allow enough signal through to obtain acceptable spectra).

The spectra for the series $\{[Ru(OEP)]_2\}^{0,1+,2+}$ show, with only minor changes, a marked similarity in vibrational frequencies and relative intensities, consistent with the oxidation occurring at the metal–metal bond and *not* at either porphyrin ligand. The similarity also implies that the porphyrin moieties are not significantly affected by changes in metal oxidation state or metal–metal bond distance. Indirect effects might have been expected because porphyrin bands often act as oxidation-state markers for the central metal in porphyrin monomers.[35,36] RR oxidation state markers for heme porphyrins include $\nu_{10}$ ("band I") and $\nu_4$ ("band IV"), but only $\nu_2$ and $\nu_{13}$ show any variation among the three dimer complexes. The reason for the insensitivity of these oxidation-state marker bands in the dimers may be related to the observed lack of sensitivity of $\pi$ back-bonding indicator modes.

Ruthenium(II) will $\pi$ back-bond equatorially into the porphyrin LUMO if no axial $\pi$ acid is present.[30,37] As the metal delocalizes $\pi$-electron density into the porphyrin LUMO, the overall porphyrin molecular wave function gains antibonding character and this will affect the force constants for the porphyrin vibrational modes. Hence, RR vibrations can act as indicators for this electronic effect. The totally symmetric mode $\nu_4$, at 1357 $cm^{-1}$ for Ru(OEP)(py)$_2$ (equatorial back-bonding to OEP) and 1371 $cm^{-1}$ for Ru(OEP)(CO) (axial back-bonding to the CO), is a key vibrational mode affected by $\pi$ back-bonding.[30] The assignment of $\nu_4$ at 1375 $cm^{-1}$ for the dimer is consistent with negligible $\pi$ back-bonding to the OEP macrocycle. Another mode shown to be sensitive to $\pi$ back-bonding is $\nu_{11}$.[38] Again, the dimer frequency (1553 $cm^{-1}$) compares more favorably to the $\nu_{11}$ stretch of Ru(OEP)(CO) (1548 $cm^{-1}$) than to that of Ru(OEP)(L)$_2$ (1535 $cm^{-1}$).[30,34] Furthermore, the dimer modes are not affected by the metal-centered oxidations, which should *decrease* the extent of $\pi$ back-bonding.

As noted above, each Ru atom of the neutral dimer is situated 0.30 Å out of the plane defined by the four coordinating nitrogen atoms in the direction of the other Ru atom. In addition, both porphyrinato cores of $\{[Ru(OEP)]_2\}^0$ have domed-type distortions.[9] These features are most likely caused by intramolecular porphyrin–porphyrin repulsion and we anticipate that a similar situation exists in $\{[Ru(OEP)]_2\}^{1+}$ and $\{[Ru(OEP)]_2\}^{2+}$. It is not unreasonable to suggest that this metal–porphyrin orientation is responsible for poor overlap of the metal $d\pi^*$ orbitals and the porphyrin $\pi^*$ orbitals and, therefore, a lack of appreciable ruthenium → porphyrin back-bonding.

Structural information about the porphyrin macrocycle is available through examination of vibrations with frequencies above 1450 $cm^{-1}$. The highest frequency skeletal $a_{2g}$ mode, $\nu_{19}$, is especially valuable in determination of the core size (other core size indicator modes include $\nu_2$, $\nu_3$, and $\nu_{10}$).[32,33,39-42] From an empirical

(31) Simic-Glavaski, B.; Tanaka, A. A.; Kenney, M. E.; Yeager, E. *J. Electroanal. Chem.* **1987**, *229*, 285–296.
(32) Oertling, W. A.; Salehi, A.; Chung, Y. C.; Leroi, G. E.; Chang, C. K.; Babcock, G. T. *J. Phys. Chem.* **1987**, *91*, 5887–5898.
(33) Oertling, W. A.; Salehi, A.; Chang, C. K.; Babcock, G. T. *J. Phys. Chem.* **1987**, *91*, 3114–3116.
(34) Schick, G. A.; Bocian, D. F. *J. Am. Chem. Soc.* **1984**, *106*, 1682–1694.
(35) Kitagawa, T.; Kyogoku, Y.; Iizuka, T.; Saito, M. I. *J. Am. Chem. Soc.* **1976**, *98*, 5169–5173.
(36) Kitagawa, T.; Abe, M.; Kyogoku, Y.; Ogoshi, H.; Sugimoto, H.; Yoshida, Z. *Chem. Phys. Lett.* **1977**, *48*, 55–58.
(37) Antipas, A.; Buchler, J. W.; Gouterman, M.; Smith, P. D. *J. Am. Chem. Soc.* **1978**, *100*, 3015–3024.
(38) Boldt, N. J.; Goodwill, K. E.; Bocian, D. F. *Inorg. Chem.* **1988**, *27*, 1188–1191.
(39) Spaulding, L. D.; Chang, C. C.; Yu, N.-T.; Felton, R. H. *J. Am. Chem. Soc.* **1975**, *97*, 2517–2525.
(40) Woodruff, W. H.; Kessler, R. J.; Ferris, N. S.; Dallinger, R. F.; Carter, K. R.; Antalis, T. M.; Palmer, G. *Electrochemical and Spectrochemical Studies of Biologic Redox Components*; Kadish, K. M., Ed.; ACS Symposium Series 201; American Chemical Society; Washington, 1982; Chapter 26.
(41) Felton, R. H.; Yu, N. T.; O'Shea, D. C.; Shelnutt, J. A. *J. Am. Chem. Soc.* **1974**, *96*, 3675–3676.
(42) Kim, D.; Su, Y. O.; Spiro, T. G. *Inorg. Chem.* **1986**, *25*, 3988–3993.

correlation of the Ct–N bond distance (i.e., the distance from the center [Ct] of the porphyrin core to a nitrogen atom) with the $\nu_{19}$ frequency, a linear plot is found: Ct–N distance (Å) = $-0.00178\nu_{19}(cm^{-1}) + 4.83$. Because this mode is located at ~1564 $cm^{-1}$ in all three dimer complexes, a Ct–N bond distance of 2.04 ± 0.01 Å can be estimated. Since each Ru atom was found to be displaced 0.30 Å out of its porphyrinic nitrogen plane in the neutral dimer,[8] the Ru–N bond length is estimated to be 2.06 ± 0.01 Å. This value is within experimental error of that previously found for the neutral dimer in the solid state (2.050 ± 0.005 Å).[8] The RR prediction that core size is relatively constant throughout this series of dimeric complexes remains to be confirmed by X-ray crystallographic studies of the oxidized dimers. The frequency of the $\nu_{19}$ band has also been correlated with the metal lying either in (1582–1609 $cm^{-1}$) or out (1552–1574 $cm^{-1}$) of the porphyrin plane.[41] A value of 1564 $cm^{-1}$ correctly predicts an out-of-plane geometry for the Ru atom in the neutral compound. Although there are exceptions to this in-plane, out-of-plane correlation,[39,41] a domed configuration for the oxidized dimers is suggested from the $\nu_{19}$ mode frequency.

Core size indicator modes contain significant $C_\alpha C_m$ contribution ($C_\alpha$ = α-pyrrole carbon; $C_m$ = methine carbon) to their normal mode description and are therefore expected to be sensitive to changes in the porphyrin $a_{2u}$ orbital, which has a large p-orbital contribution from $C_m$.[20,21] Direct overlap of the two porphyrin $a_{2u}(\pi)$ orbitals upon dimerization should then significantly change the frequencies of these modes.[20,21] However, the frequencies of these modes in the dimers are similar to those found in the Ru(OEP)(CO) complex (see Table II), implying a lack of π overlap of the $a_{2u}$ orbitals upon dimerization. Such an effect has been reported previously for π–π dimer porphyrins, where only the $a_{1u}(\pi)$ orbitals interact.[20,21]

As mentioned above, the monochromator slits were opened rather wide. This was required because the Raman scattering of all three complexes is remarkably weak (unusual for metalloporphyrin complexes). Similarly weak Raman scattering intensity has been noted previously for π–π dimer porphyrins.[20a] The reasons for this are not clear. We have demonstrated that, because strong solvent signals are observed, this is an intrinsic property of these systems rather than an experimental artifact due to poor alignment or reabsorption. The broad range of excitation wavelengths used would also rule out an antiresonance deenhancement mechanism.[43] Because the absorption bands are broad, a small displacement of the excited state cannot account for the weak scattering. Moreover, non totally symmetric modes that do not derive their enhancement from the Franck–Condon mechanism are involved. A possible explanation for the weak Raman scattering is the presence of a low-energy excited state, relaxation into which may significantly shorten the lifetimes of the porphyrin-centered excited states.[44]

**II. Infrared Absorption Studies.** The IR absorption spectrum for Ru(OEP)(CO) in $CH_2Cl_2$ exhibits a strong carbonyl stretch at 1920 $cm^{-1}$, shifted from 2155 $cm^{-1}$ for free CO.[45] This observation indicates considerable axial π back-bonding. In the mid-IR region (800–1650 $cm^{-1}$), the porphyrin-based IR active vibrations for the monomeric species are either $e_u$ in-plane modes of the porphine skeleton or ethyl group vibrations. Out-of-plane $a_{2u}$ modes (nominally IR active) are not usually observed.[45,46] In general, the IR absorption bands can be correlated with those found in Ni(OEP) (see Table III), where the vibrational descriptions have been previously assigned.[46] In addition to these fundamental porphyrin IR bands, other weak absorption bands for Ru(OEP)(CO) occur at 1187, 1305, 1365, and 1539 $cm^{-1}$. These bands correlate with unassigned bands on other metal octaethylporphyrins[46,47] and are identified as combination/overtone bands.

The IR spectra for the cationic dimer complexes were also recorded. Spectra were obtained only for the oxidized dimers

**Table III.** IR Bands of Ni(OEP), Ru(OEP)(CO), and $\{[Ru(OEP)]_2\}^{n+}$ (in $CH_2Cl_2$)

| Ni(OEP)[a] | monomer | n = 1 | n = 2 | | assignment |
|---|---|---|---|---|---|
| 834 | 830 | | 824 | | π($C_mH$) |
| 846 | 847 | 854 | 854 | | π($C_mH$) |
| 927 | 921 | 922 | 922 | $\nu_{46}$ | {ν($C_\alpha C_m$), ν($C_\beta C_S$)} |
| 959 | 960 | 961 | 960 | | ethyl group |
| 996 | 991 | 992 | 992 | $\nu_{45}$ | {ν($C_\alpha N$), ν($C_\alpha C_m$)} |
| 1021 | 1019 | 1017 | 1016 | | ethyl group |
| | | 1038 | 1038 | | $BF_4^-$ [b] |
| 1061 | 1058 | 1056 | 1056 | | ethyl group |
| 1069 | 1064 | | | | ethyl group |
| | | 1094 | 1094 | | $BF_4^-$ [b] |
| 1119 | 1110 | 1112 | 1110 | | ethyl group |
| 1133 | | (1125) | | $\nu_{44}$ | {ν($C_\alpha N$), δ($C_\alpha C_m H$)} |
| 1153 | 1149 | 1148 | 1148 | $\nu_{43}$ | {ν($C_\alpha N$), δ($C_\alpha C_m H$)} |
| | (1187) | | | | |
| 1231 | 1229 | 1221 | | $\nu_{42}$ | {ν($C_\alpha N$), δ($C_\alpha C_m H$)} |
| 1275 | S[c] | (1272) | 1272 | $\nu_{41}$ | {ν($C_\alpha C_\beta$), ν($C_\beta C_\beta$)} |
| | 1305 | (1294) | 1287 | | |
| 1323 | 1317 | 1317 | 1314 | | ethyl group |
| | 1365 | 1363 | 1362 | | |
| 1378 | 1379 | 1378 | 1378 | | ethyl group |
| 1396 | | 1390 | 1391 | $\nu_{40}$ | {ν($C_\alpha C_\beta$), ν($C_\beta C_S$)} |
| 1456 | 1453 | 1453 | 1453 | | ethyl group |
| 1473 | 1467 | 1467 | 1467 | | ethyl group |
| | | 1480 | | | |
| 1501 | | 1499 | 1501 | $\nu_{39}$ | ν($C_\alpha C_m$) |
| | 1538 | | | | |
| 1575 | 1551 | 1554 | 1553 | $\nu_{38}$ | ν($C_\alpha C_m$) |
| 1604 | 1600 | 1594 | | $\nu_{37}$ | ν($C_\beta C_\beta$) |

[a] Reference 46. ν, stretch; δ, in-plane deformation; π, out-of-plane deformation. [b] Reference 49. [c] S, solvent interference.

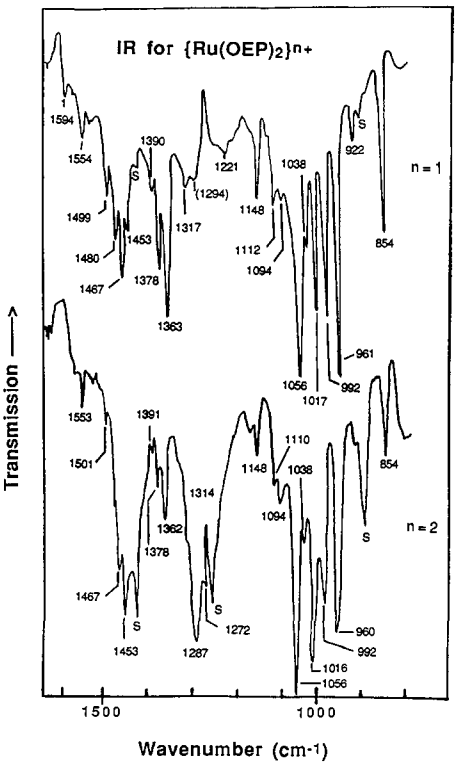


**Figure 7.** IR transmission spectra for $\{[Ru(OEP)]_2\}^{n+}$ (n = 1 and 2) in $CH_2Cl_2$.

(43) Nafie, L. A.; Pastor, R. W.; Dabrowiak, J. C.; Woodruff, W. H. *J. Am. Chem. Soc.* **1976**, *98*, 8007–8014.
(44) Gouterman, M.; Aranowitz, S.; Adar, F. *J. Phys. Chem.* **1976**, *80*, 2184–2191.
(45) Nakamoto, K. *Infrared and Raman Spectra of Inorganic and Coordination Compounds*, 4th ed.; Wiley: New York, 1986.
(46) Kincaid, J. R.; Urban, M. W.; Watanabe, T.; Nakamoto, K. *J. Phys. Chem.* **1983**, *87*, 3096–3101.
(47) Ogoshi, H.; Masai, N.; Yoshida, Z.; Takemoto, J.; Nakamoto, K. *Bull. Chem. Soc. Jpn.* **1971**, *44*, 49–51.

(Figure 7) because the available solvents for the neutral dimer could not be used, either because of chemical problems ($CS_2$) or because of IR absorption interference (THF). As in the Raman spectra, the observed dimer IR frequencies are compared with those of monomeric compounds (Table III).

The question of $\pi$-system interaction between the porphyrin rings of the dimers motivated the IR data collection. Such $\pi$-system interactions may be detected in the vibrational spectra in three ways. First, as mentioned above, core size indicator modes, which have $C_\alpha C_m$ character, will shift considerably if the $a_{2u}(\pi)$ orbitals overlap.[20,21] Second, with the additional presence of vibronic coupling between excitonically coupled states, doublets in the RR vibrational bands may be observed.[15] However, as mentioned above, no such doubling was found. Finally (and most sensitively), with no exclusion rule of RR and IR activity in the noncentrosymmetric dimer, a mode that is Raman active in the corresponding monomer can become IR active as the out-of-phase combination in the dimer.[16,17] Similarly, an IR active (in-phase) mode may become RR active as the out-of-phase combination. Coupling between the $\pi$ systems drives apart the frequencies of the two modes (in- and out-of-phase) and increases the "allowedness" of the out-of-phase mode in each spectroscopy.

To this end, note that no doubling of peaks is evident despite the 2-$cm^{-1}$ resolution of the FTIR spectrometer. Almost every dimer IR peak in Table III can be matched with peaks from the Ni(OEP) and Ru(OEP)(CO) IR spectra. However, a peak at 1480 $cm^{-1}$, not present in either of the monomers, appears for the $\{[Ru(OEP)]_2\}^{1+}$ complex. The appearance of this dimer-unique IR band near the location of a RR band ($\nu_3$ at 1482 $cm^{-1}$) could indicate $\pi$-system coupling. However, the near coincidence of the peak frequencies more likely suggests that it is a result of increased coupling facilitated by the high order Ru–Ru bonds and not direct $\pi$-orbital overlap. A similar rationale was invoked to explain the coincidence of several IR and RR active modes in the aforementioned nitrogen-bridged iron porphyrin dimer.[17] Hence, while the electronic absorption spectra for the dimers indicate excitonic coupling (vide supra), evidence from the vibrational spectra suggests that *ground-state* porphyrin $\pi$-orbital overlap is not significant. The low energy barriers expected for rotation about the metal–metal bond axis should also be noted.[48] Facile rotation about the M–M bond is further evidence that intramolecular interactions between porphyrin macrocycles are very weak (or nonexistent). Severe doming of the $RuN_4$ units is a reasonable explanation for poor overlap of the $\pi$ orbitals.

As in the RR active vibrations, the IR active frequencies are remarkably similar for all of the Ru(OEP) complexes and, in general, close to the frequencies observed for the Ni(OEP) compound. Of the metal-sensitive modes ($\nu_{38}$, $\nu_{39}$, $\nu_{42}$, and $\nu_{45}$),[46] only $\nu_{38}$ is substantially different between the Ru and Ni compounds. This constancy of the predominately $C_\alpha C_m$ stretches is unexpected, since pyrrole tilting, as occurs in the domed Ru complexes, changes the bond strength of the methine bridge when compared to the planar arrangement of Ni(OEP).[46] Moreover, the overall constancy of the IR vibrational frequencies for the Ru complexes implies, as did the RR active vibrations, little perturbation of the porphyrin macrocycles by the oxidation-state changes.

## Conclusions

The increase in the Ru–Ru stretching frequency (285 → 301 → 310 $cm^{-1}$) as electrons are successively removed from the metal–metal bond of $[Ru(OEP)]_2$ provides direct vibrational evidence for the bonding scheme previously proposed.[8,9] Removal of electron density from the metal–metal $\pi^*$ anti-bonding orbitals has little effect on the porphyrin-centered RR and IR spectra, suggesting little change in the structural parameters of the macrocycle upon oxidation. Although the UV/vis spectra support the existence of excitonic coupling between the two porphyrin ligands, little vibrational evidence for ground-state $\pi$-orbital interaction is found.

**Acknowledgment.** The spectroscopic work was performed at Los Alamos National Laboratory under the auspices of the U.S. Department of Energy, supported by a LANL Institutional Supporting Research Grant to W.H.W., and an Office of Energy Research, Division of Chemical Sciences Grant to A.P.S. C.D.T. gratefully acknowledges the support of the Director's Fellowship Program at LANL. We also thank Drs. Robert J. Donohoe and Edward M. Kober for helpful discussions and suggestions, and one of the reviewers for some insightful comments. The synthetic work at Stanford was supported by the National Science Foundation (NSF CHE83-18512) and the National Institutes of Health (GM17880-15,16). J.M.G.'s portion of this work is dedicated to his father, James H. Garner.

**Registry No.** $\{[Ru(OEP)]_2\}^0$, 54762-43-5; $\{[Ru(OEP)]_2\}^+$, 101494-42-2; $\{[Ru(OEP)]_2\}^{2+}$, 101658-45-1; Ru(OEP)(CO), 41636-35-5; Ru, 7440-18-8.

(48) Previous NMR experiments have shown that the rotation about the Mo–Mo quadruple bond of meso-substituted molybdenum(II) porphyrin dimers is a remarkably facile process at ambient temperature. See: Collman, J. P.; Woo, L. K. *Proc. Natl. Acad. Sci. U.S.A.* **1984**, *81*, 2592–2596.

(49) Greenwood, N. N. *J. Chem. Soc.* **1959**, 3811–3815.